Journal of Nuclear Materials 377 (2008) 470–475

Contents lists available at ScienceDirect

Journal of Nuclear Materials

journal homepage: www.elsevier.com/locate/jnucmat

Pyrochlore-structured titanate ceramics for immobilisation of actinides: Hot isostatic pressing (HIPing) and stainless steel/waste form interactions

Yingjie Zhang *, Huijun Li, Sam Moricca

Institute of Materials and Engineering Science, Australian Nuclear Science and Technology Organisation, Menai, NSW 2234, Australia

ARTICLE INFO

Article history:
Received 5 June 2007
Accepted 12 March 2008

ABSTRACT

A pyrochlore-structured titanate ceramic has been studied in respect of its overall feasibility for immobilisation of impure actinide-rich radioactive wastes through the hot isostatic pressing (HIPing) technique. The resultant waste form contains mainly pyrochlore (~70%), rutile (~14%) as well as perovskite (~12%), hollandite (~2%) and brannerite (~1%). Optical spectroscopy confirms that uranium (used to simulate Pu) exists mainly in the stable pyrochlore-structured phase as tetravalent ions as designed. The stainless steel/waste form interactions under HIPing conditions (1280 °C/100 MPa/3 h) do not seem to change the actinide-bearing phases and therefore should have no detrimental effect on the waste form.

1. Introduction

Over the past 30 years, Synroc-C (an assemblage of geologically stable titanate minerals) and its derivatives have been extensively studied [1–6], both in the laboratory and via natural analogue minerals, as potential candidates for immobilisation of high-level radioactive wastes ranging from reprocessed spent fuel to impure plutonium derived from nuclear weapons programs. Depending upon the natures of the waste streams, titanate ceramic formulations have evolved from the original polyphase assemblages to deal with a wide range of fission products, actinides and process chemicals, to more specific compositions for partitioned fission products or actinides. These latter waste forms are largely based on a major phase, e.g., brannerite [7,8], hollandite [9], zirconolite [10,11] and pyrochlore [12,13], etc. Pyrochlore-rich ceramics are among the specific compositions developed initially for immobilisation of surplus impure plutonium using sintering as the consolidation process [14] and have since been tailored to suit various actinide-rich waste streams. Nevertheless, all these waste forms contain sufficient amounts of targeted additional phases to allow compositional flexibility to deal with variations in waste chemistry and waste/precursor ratio [12,13].

Pyrochlore is a derivative of the fluorite structure and has the general formula $A_2B_2X_6Y$, in which A and B are 8- and 6-coordinated cation sites, and X and Y are 4-coordinated anion sites [15]. In general, Na, Ca, Y, lanthanides and actinides can be incorporated on the A site, and Ti, Zr, Nb, Hf, Ta, Sn and W can be incorporated on the B site. Recent studies have revealed that even fully amorphous titanate pyrochlore samples (^{238}Pu-doped) have very similar dissolution rates as those of the corresponding crystalline samples [12,13], showing that the chemical durability of the pyrochlore structure is sustained even when it is fully amorphous due to radiation damage.

As one of the advanced ceramic processing methods, hot isostatic pressing (HIPing) has been extensively studied in the past 10 years [16]. It has many obvious advantages over the conventional methods (such as sintering or melting) for processing of high-level radioactive wastes, notably no radioactive volatile emissions in the high temperature consolidation step (very important for wastes containing fission products which would be volatile on hot consolidation) due to the closed processing system, less secondary waste and flexible processing conditions [17]. Several industry-scale HIPing systems are currently being set up for processing of actinide-rich radioactive wastes [18,19]. At HIPing conditions (high temperatures and high pressure), the waste form and the stainless steel container used for containment of the waste form may potentially interact, which may in turn result in some detrimental effects on the quality of the waste form. Previously we have reported such interactions for an early Synroc sample containing mainly zirconolite, hollandite and rutile [17]. It is of interest and important to understand such interactions for pyrochlore-rich formulations as currently they are eminently amenable to high actinide waste loadings.

In the present study, a pyrochlore-rich formulation was chosen to test its overall feasibility for immobilisation of actinide-rich radioactive wastes (using U as a surrogate for Pu) through HIP processing, including characterisations of actinide-bearing phases, actinide valences, stainless steel can/waste form interactions under HIPing conditions and chemical durability of the waste form.

---

* Corresponding author. Tel.: +61 2 9717 9156; fax: +61 2 9543 7179.
E-mail address: Yingjie.Zhang@ansto.gov.au (Y. Zhang).

0022-3115/$ - see front matter © 2008 Elsevier B.V. All rights reserved.
doi:10.1016/j.jnucmat.2008.03.022

1.1. Justification and limitations of using U as a surrogate for Pu

The ideal candidates for simulating Pu in the current context would have similar chemistry, valence and ionic sizes. The surrogates widely being used are Ce, Zr, Hf, U and Th. Of these, Ce is a very popular non-radioactive choice because of its similar ionic size and redox state. U and more particularly Th are the best mildly radioactive simulants for ionic size and stability of tetravalent state under reducing conditions. Unlike UO_2 and ThO_2, CeO_2 and PuO_2 are readily reduced at elevated temperatures to form oxygen-deficient fluorite-structured compounds containing trivalent metal ions as well as tetravalent ions [20,21].

Our previous work [17] suggests action on the can material by the ceramic is mainly a redox effect with the can at the interface being oxidised by the presence of the oxide ceramic. Cr and Fe from the can interact with Ti-rich oxides to form Cr and Fe oxides, mainly Cr oxide. On the other hand, the obvious influence of the can on the oxide ceramic is to reduce actinides as well as the Ti oxides.

It is well known that Pu adopts tetravalent state in the oxide ceramics designed for immobilisation of surplus Pu under air and argon sintering conditions [22]. From the chemical design point of view, Pu has been targeted to be in tetravalent state in the current formulation. Under HIP conditions, Pu would be most likely in the tetravalent state in the main ceramic matrix. However, trivalent Pu ions may exist in the interface area similarly as the presence of detectable trivalent Pu ions in a zirconolite preparation under reducing conditions [22]. With U (or Th) as a surrogate for Pu, there is no way to produce trivalent U ions in oxide ceramics. Moreover, the formation of trivalent Pu ions in the oxide ceramic might change the pyrochlore phase to zirconolite plus another phase or simply generate oxygen vacancies in the pyrochlore at the reaction interface.

It is comprehensible that Pu and U have very similar chemical durability trends both in short-term and long-term in pyrochlore samples in which U replaces some of the Pu [23]. In addition, it has been demonstrated that trivalent and tetravalent Pu ions have similar chemical durability in oxide ceramics [23]. Therefore U is an appropriate surrogate for Pu regards to both similar chemistry and chemical durability.

2. Experimental

A titanate ceramic formulation was designed for immobilisation of impure Pu or partitioned actinide-rich radioactive wastes which may contain small amounts of fission products. It was developed based on the pyrochlore-structured phase to incorporate actinides, hollandite and perovskite to accommodate fission products Cs and Sr, etc. The detailed oxide composition is given in Table 1. The sample was prepared by the alkoxide/nitrate route [1], calcined in 3.5% H_2/N_2 at 750 °C for 1 h and then hot isostatically pressed (HIPed) at 1280 °C, 100 MPa for 3 h under an argon atmosphere. The HIP-can was made from 2 mm thick 316 stainless steel.

Table 1
Calculated oxide composition (wt%) of the pyrochlore-rich formulation

Oxide	wt%
Al_2O_3	1.7
BaO	3.4
CaO	11.9
Cs_2O	0.1
Fe_2O_3	0.2
MgO	0.1
SrO	0.1
TiO_2	43.6
UO_2	35.0
ZrO_2	3.9

A polished sample was prepared for characterisation of phases formed in the bulk material. An interface sample was cut for characterisation of the interactions between the stainless steel and the waste form after HIPing. Special care was taken to prevent the delamination of the waste form from the can. The sample was then mounted in epoxy resin, and polished to a 0.25 μm diamond finish.

Specimens (8 × 8 × 2 mm) for durability testing of the bulk waste form were prepared and polished to a 0.25 μm diamond finish. The durability tests were carried out at 90 °C in duplicate in deionised water, according to the ASTM static leaching protocol [24]. The leachate were analysed by ICP–MS (inductively coupled plasma–mass spectrometry) for elemental releases.

Scanning electron microscopy (SEM) on polished and interface samples was carried out on a JEOL 6400 instrument run at 15 kV and fitted with a Tracor Northern TN5502 energy-dispersive spectrometer (EDS) which utilised a comprehensive range of standards for quantitative work [25].

Diffuse reflectance spectra were collected at ambient temperature using a Cary 500 spectrophotometer equipped with a Labsphere Biconical Accessory. Spectra are referenced to that of a Labsphere certified standard (Spectralon), and transformed into Kubelka–Munk units, $F(R) = (1 - R)^2/2R$ [26].

3. Results

3.1. Characterisation of the waste form

The backscattered electron image of the bulk waste form is shown in Fig. 1. In essential accordance with its design, it contains mainly pyrochlore (~70%), rutile (~14%) as well as perovskite (~12%), hollandite (~2%), brannerite (~1%) and zirconolite (<1%). Note the typical grain sizes are less than 4 μm for perovskite, hollandite and brannerite, and from a few μm up to 50 μm for rutile. The average oxide compositions of pyrochlore, hollandite, perovskite and brannerite are shown in Table 2, although the exact compositions of perovskite, hollandite and brannerite were difficult to determine due to the very small grain size. It is emphasised that minimum grain size is an advantage to maximise mechanical

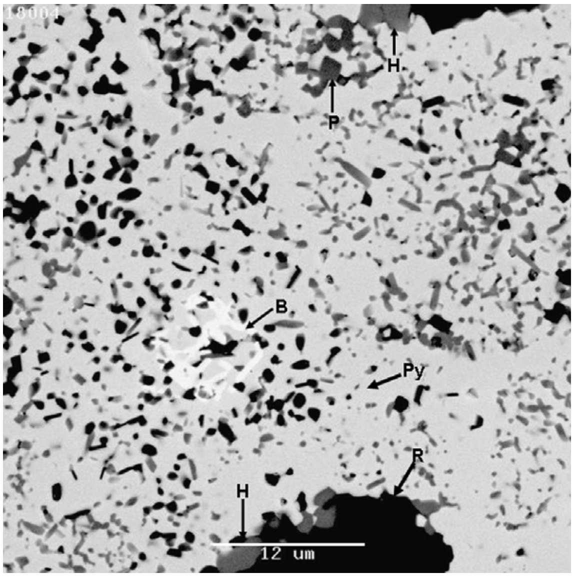

Fig. 1. SEM backscattered electron image of the polished sample shows mainly pyrochlore (Py) plus minor hollandite (H), rutile (R) and small amounts of brannerite (B) and perovskite (P).

Table 2
Average main oxide compositions (wt%) of pyrochlore, hollandite, perovskite and brannerite phases in the pyrochlore-rich ceramic waste form

Oxide	Pyrochlore (wt%)	Hollandite (wt%)	Perovskite (wt%)	Brannerite (wt%)
Al_2O_3	1.2	7.5	0.9	0.1
BaO	0.1	19.1		0.1
CaO	11.6	0.2	33.2	0.4
Cs_2O		0.9		
FeO	0.2	0.4	0.1	
SrO		0.2	0.3	
TiO_2	39.4	70.7	54.0	40.6
UO_2	42.7	0.5	10.2	55.0
ZrO_2	3.7	0.2		2.8

durability. The majority of uranium has been incorporated in the pyrochlore structure as designed, with only small amounts of uranium in perovskite and brannerite. Cs partitioning in hollandite is apparently not as good as expected, but this is partly an artefact due to the very small grain size for hollandite (see below).

3.2. Characterisation of the interface region between HIP-can and waste form

The SEM backscattered electron image of the cross-sectional interface region shown in Fig. 2 reveals several distinctive layers between the stainless steel HIP-can and the waste form. X-ray elemental mapping was performed in the same region (shown in Fig. 3) to assist SEM–EDS analysis for detailed interpretation of the reaction interface.

Layer 1 (marked on Fig. 2) is the interior edge of the stainless steel can adjacent to the reaction interface. The EDS analysis showed no obvious elemental depletion. Some scattered Cr oxide and SiO_2 particles (<3 μm in diameter) well away from the reaction interface are also present in this layer (see Fig. 3). Small SiO_2 particles along the reaction interface on the stainless steel side of HIPed waste forms have been observed previously [27] and they appear to be the result of oxidation and migration of trace amounts of Si in 316 stainless steel (typical composition: Fe: 61.8–68.8%, C: 0.08%; Mn: 2.0%; P: 0.045%, S: 0.03%, Si: 1.0%, Cr: 16–18%, Ni: 10–14%, Mo: 2–3%) towards the reaction interface.

Layer 2 is mainly Cr-rich oxide (see Figs. 2 and 3, >95% of Cr_2O_3 from EDS analysis) resulting from the diffusion of other stainless steel components out of Layer 2 towards the waste form and subsequent oxidation of the can material adjacent to the waste form. The composition is very uniform throughout the layer and the thickness of the layer varies from 2 to 10 μm. This is the oxidation front of the stainless steel can.

Layer 3 contains Cr- and Fe-rich oxides derived from oxidation of the stainless steel can and the compositions vary significantly with the distance from Layer 2 (see Figs. 3 and 4) towards the waste form. The thickness of this layer varies from a few to over 30 μm. Significant amounts of Al and small amounts of Ti were found in this layer (see Figs. 3 and 4), as the result of Al and Ti (from hollandite and rutile) diffusion from the waste form.

Layer 4, ranging from a few to 20 μm in thickness, is a fairly uniform oxide layer rich in Ti with some Fe and Cr (see Table 3), formed as a result of direct reaction between the oxidised stainless steel and the waste form. Layer 3 and Layer 4 together form the can/waste form interface.

Layer 5 is the front of pyrochlore phase showing different microstructures compared to the bulk material (see Figs. 2 and 3) with much less rutile and hollandite phase abundance. The chemical composition of pyrochlore in Layer 5 is similar to that of the matrix pyrochlore but contains trace amounts of Fe and Cr. Small metallic particles (⩽5 μm) containing Ni, Cr, Fe and Mo spread out from Layer 3 to Layer 5 (see Fig. 3).

It is apparent that the pyrochlore-rich waste form/HIP-can interactions involve diffusion of Fe/Cr from stainless steel and Al/Ti from the waste form (from hollandite and rutile), forming mixed oxide solid solutions in Layers 3 and 4.

In the previous study [17] on the synroc/HIP-can interactions, Fe has been proven to be the main element diffusing from the HIP-can into synroc waste form for about 300 μm, replacing Ca/Ti in zirconolite and replacing Al in hollandite. However, in the current work on the pyrochlore-rich waste form/HIP-can interactions, there is no indication of diffused Fe from the HIP-can being incorporated in the pyrochlore-rich waste form. Instead Al-/Ti-rich phases (hollandite and rutile) from the pyrochlore-rich waste form diffuse to the interface region and form mixed oxide solid solutions with Fe and Cr from the HIP-can.

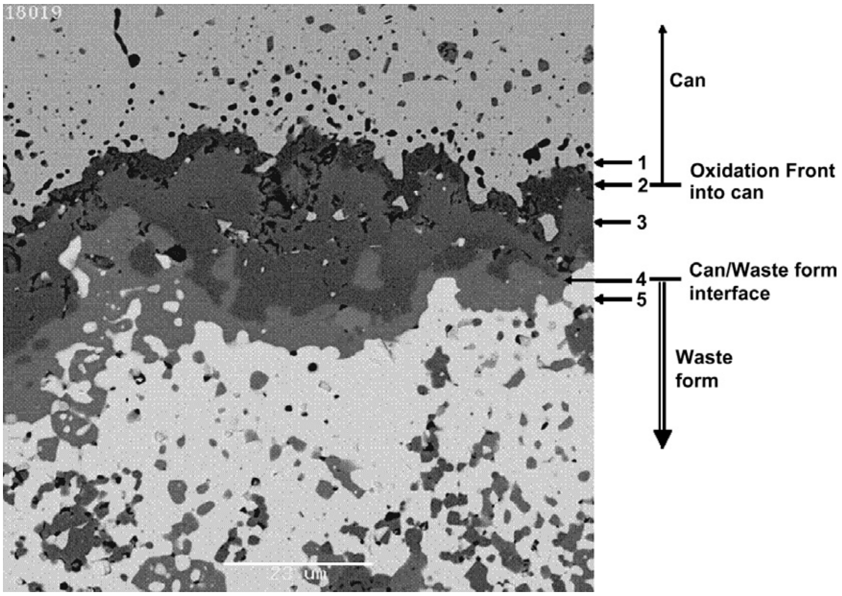

Fig. 2. SEM backscattered electron image of the cross-sectional interface shows three distinguished reaction layers between the stainless steel can and the pyrochlore-rich waste form.

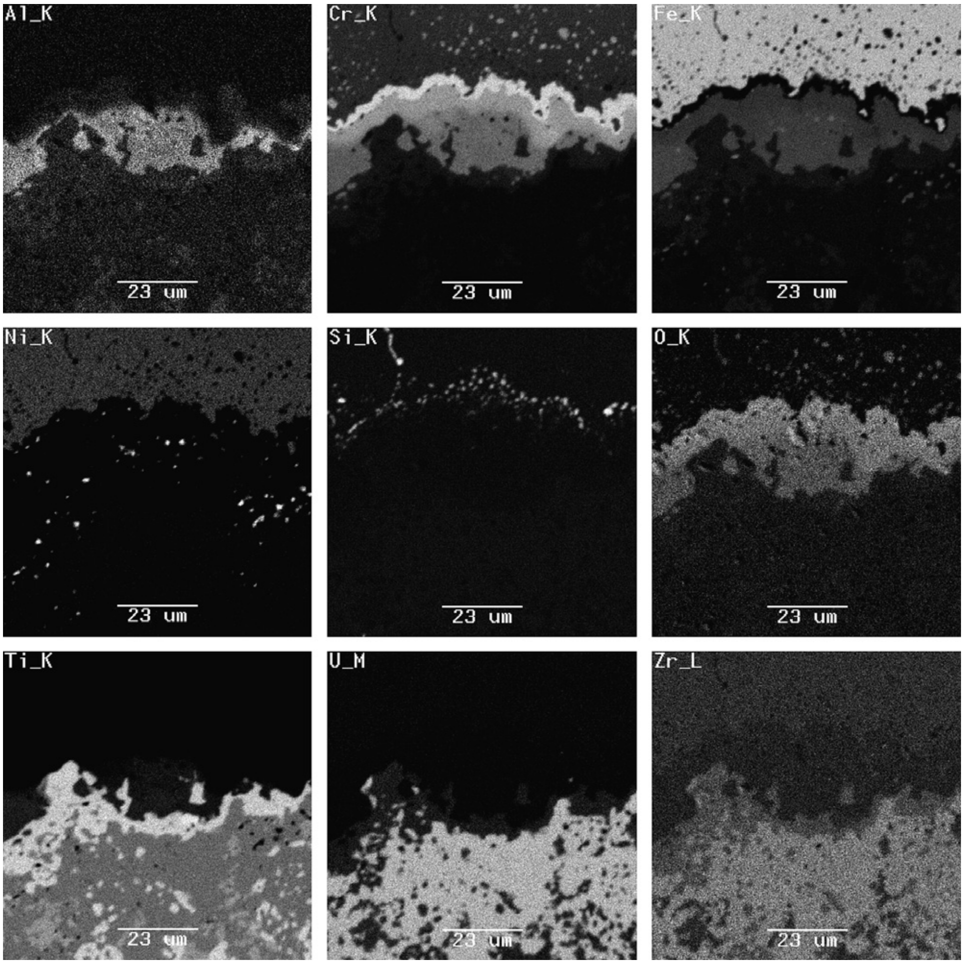

Fig. 3. Cross-sectional X-ray mapping of the interface region. The lighter the colour, the more abundant is the element.

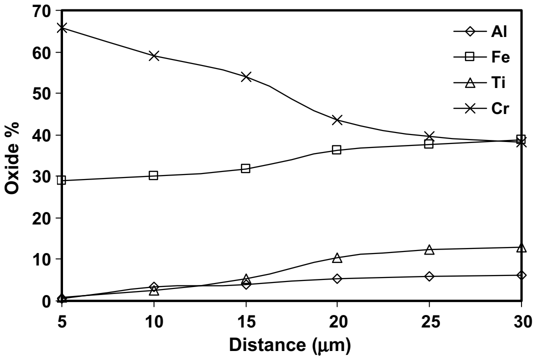

Fig. 4. Elemental profiles of oxide in layer 3 from the edge of layer 2 towards the waste form.

Table 3
Oxide composition (wt%) of layer 4

Oxide	Al_2O_3	BaO	CaO	Cr_2O_3	FeO	MnO	SrO	TiO_2	UO_2	ZrO_2
wt%	1.7	3.4	2.2	9.5	10.4	1.4	0.3	60.3	7.2	2.3

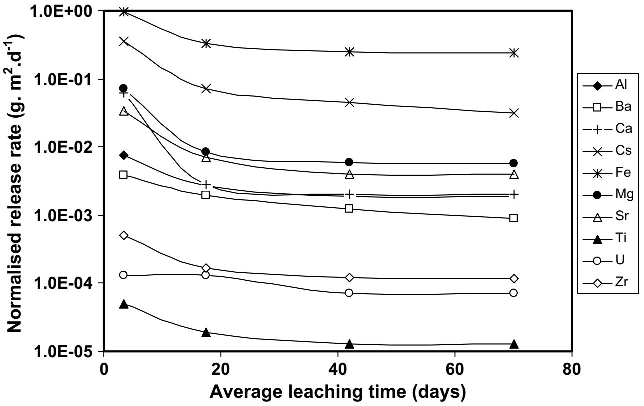

Fig. 5. Normalised release rates (g m^2 d^{-1}) versus average leaching time for the waste form leached in deionised water at 90 °C. Upper limits were used for Cs, Fe, Mg and Sr since their concentrations in leachates were all below detection limits of the instrument.

3.3. Chemical durability of the waste form

Fig. 5 shows the normalised elemental release rates against average leaching time for the bulk waste form leached in deionised water at 90 °C for 1, 7, 28, 56 and 84 days. The releases of minor elements such as Cs, Fe, Mg and Sr are all well below the detection limits and the upper limits are being used in Fig. 5. The upper limits of Cs release rates are very comparable with those of synroc-C for short times [4], suggesting no leachable Cs phases are present.

In general, the dissolution of the waste form is not stoichiometric, with normalised release rates of Al, Ba and Ca being about one and a half orders of magnitude higher than those of U, Zr and about two orders of magnitude higher than that of Ti. The relative stability of the phases with which these elements are associated is broadly consistent with the incongruent dissolution nature of the waste form, e.g. Al and Ba are mainly in hollandite, some Ca is in perovskite and U is mainly in pyrochlore and brannerite. The current results on chemical durability of the pyrochlore-rich waste form are broadly consistent with those of the previously studies on synroc-C [4] and zirconolite-rich ceramics [6].

A systematic study on some natural pyrochlores revealed that natural samples alter by cation exchange [5] upon exposure to water and the A-site cation mobility is largely determined by valence and ionic radius constraints. As a result, the observed mobility sequence of A-site cations in natural pyrochlores is Na > Ca > Sr > Ba > REEs > Th, U. It is important to note that the results of chemical durability testing on the pyrochlore-rich waste form here are broadly consistent with the observed mobility sequence of A-site cations in natural pyrochlores, suggesting cation exchange as the main chemical alteration mechanism.

Although it has been demonstrated through inactive leaching [28] of a glass-ceramic sample that the interface materials have little effect on the overall chemical durability of the waste form, it is still imperative to study further and understand better the interface material to confirm that. However, it has not been considered in this study mainly due to technical difficulties to peel off the HIPed can without damaging the interface region and to eliminate the contribution from the bulk waste form as well.

3.4. Characterisation of U valence state

Diffuse reflectance spectra of uranium ions in polycrystalline titanate phases, e.g. brannerite, provskite, zirconolite and pyrochlore have been reported previously [29,30]. It is evident that tetravalent and pentavalent uranium ions in different phases have distinctive characteristic spectral features due to different site symmetries [30]. Therefore diffuse reflectance spectra can be used to identify uranium valences.

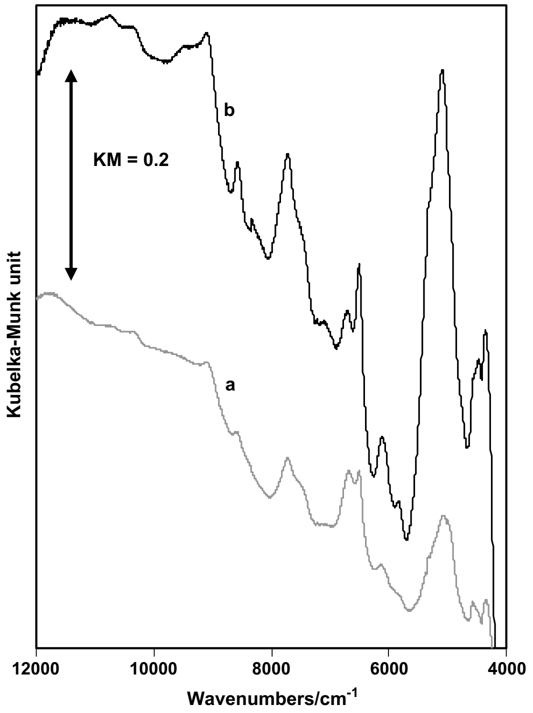

Fig. 6. Diffuse reflectance spectra (4000–12 000 cm^{-1}) of (a) a single-phase pyrochlore sample ($Ca_{0.89}Zr_{0.11}U_{0.67}Cd_{0.05}Ce_{0.05}La_{0.06}Nd_{0.06}Hf_{0.11}Ti_2O_7$) and (b) the bulk waste form.

Diffuse reflectance spectra of the bulk waste form together with that of a single-phase pyrochlore ($Ca_{0.89}Zr_{0.11}U_{0.67}Cd_{0.05}Ce_{0.05}La_{0.06}Nd_{0.06}Hf_{0.11}Ti_2O_7$), in the near infrared range, are shown in Fig. 6. The similarity of the two spectra suggests that majority of uranium is present as tetravalent ions in pyrochlore, consistent with the above SEM observations. It would be expected that Pu^{4+} would exhibit similar partitioning to U^{4+}, but the partitioning of Pu^{3+} is still somewhat uncertain.

4. Conclusion

For the pyrochlore-structured waste form considered here, the HIP-can/waste form interactions under HIPing conditions do not seem to change the actinide-bearing phase distribution or produce any obviously undesirable phases at the interface. As designed, uranium exists as mainly tetravalent ions in the durable pyrochlore-structured major phase in the waste form. Overall, pyrochlore-rich formulations are very suitable for immobilisation of impure actinide-rich wastes due to their chemical durability and high actinide waste loadings.

Acknowledgements

We are indebted to K. Olufson for durability testing, P. Yee for ICP–MS analysis and E.R. Vance for helpful discussion and valuable comments to improve the manuscript.

References

[1] A.E. Ringwood, S.E. Kesson, K.D. Reeve, D.M. Levins, E.J. Ramm, in: W. Lutz, R.C. Ewing (Eds.), Radioactive Waste Forms for the Future, North-Holland, Amsterdam, 1988, p. 233.
[2] E.R. Vance, MRS Bull. XIX (2) (1994) 28.
[3] G.R. Lumpkin, K.L. Smith, M.G. Blackford, J. Nucl. Mater. 224 (1995) 31.
[4] K.L. Smith, G.R. Lumpkin, M.G. Blackford, R.A. Day, J. Nucl. Mater. 190 (1992) 287.
[5] G.R. Lumpkin, R.C. Ewing, Am. Mineral. 80 (1995) 732.
[6] Y. Zhang, K.P. Hart, W.L. Bourcier, R.A. Day, M. Colella, B. Thomas, Z. Aly, A. Jostsons, J. Nucl. Mater. 289 (2001) 254.
[7] Y. Zhang, B. Thomas, G.R. Lumpkin, M. Blackford, Z. Zhang, M. Colella, Z. Aly, J. Nucl. Mater. 321 (2003) 1.
[8] Y. Zhang, G.R. Lumpkin, H. Li, M. Colella, M.L. Carter, E.R. Vance, J. Nucl. Mater. 350 (2006) 293.
[9] M.L. Carter, R.L. Withers, J. Solid State Chem. 178 (2005) 1903.
[10] B.D. Begg, E.R. Vance, B.A. Hunter, J.V. Hanna, J. Mater. Res. 13 (11) (1998) 3181.
[11] E.R. Vance, G.R. Lumpkin, M.L. Carter, D.J. Cassidy, C.J. Ball, R.A. Day, B.D. Begg, J. Am. Ceram. Soc. 85 (6) (2002) 1853.
[12] J.P. Icenhower, D.M. Strachan, B.P. McGrail, R.D. Scheele, E.A. Rodriquez, J.L. Steele, V.L. Legore, Am. Mineral. 91 (2006) 39.
[13] D.M. Strachan, R.D. Scheele, E.C. Buck, J.P. Icenhower, A.E. Kozelisky, R.L. Sell, R.J. Elovich, W.C. Buchmiller, J. Nucl. Mater. 345 (2005) 109.
[14] Y. Zhang, K.P. Hart, M.G. Blackford, B. Thomas, Z. Aly, G.R. Lumpkin, M.W.A. Stewart, P.J. McGlinn, A. Brownscombe, Mat. Res. Soc. Symp. Proc. 663 (2001) 325.
[15] G.R. Lumpkin, Elements 2 (2006) 365.
[16] B.D. Begg, R.A. Day, S. Moricca, M.W.A. Stewart, E.R. Vance, Low-risk waste forms to lock up high-level nuclear waste, in: WM'05 Conference, February 27–March 3, 2005, Tucson, AZ, USA.
[17] H. Li, Y. Zhang, P.J. McGlinn, S. Moricca, B.D. Begg, E.R. Vance, J. Nucl. Mater. 355 (2006) 136.
[18] ANSTO Media Release: 'Liquid waste to turn rock-solid in world-first', Australian Nuclear Science and Technology Organisation, 6 September 2005.
[19] ANSTO Report, R06m057, Australian Nuclear Science and Technology Organisation, 19 June 2006.
[20] D.C. Hoffman, Advances in Plutonium Chemistry, 1967–2000, American Nuclear Society, 2002.
[21] O. Toft Sørensen, J. Solid State Chem. 18 (1976) 217.
[22] B.D. Begg, E.R. Vance, R.A. Day, M. Hambley, S.D. Conradson, Mat. Res. Soc. Symp. Proc. 465 (1997) 325.
[23] E.R. Vance, A. Jostsons, S. Moricca, M.W.A. Stewart, R.A. Day, B.D. Begg, M.J. Hambley, K.P. Hart, B.B. Ebbinghaus, Environmental issues and waste management technologies in the ceramic and nuclear industries XI, in:

Proceedings of the 107th Annual Meeting of The American Ceramic Society, Baltimore, Maryland, USA 2005, Ceramic Transactions, vol. 176, p. 323.

[24] ASTM C 1220–98, Standard Test Method for Static Leaching of Monolithic Waste forms for Disposal of Radioactive Waste, ASTM International, 1998.

[25] G.R. Lumplin, K.L. Smith, M.G. Blackford, R. Giere, C.T. Williams, Micron 25 (6) (1994) 581.

[26] W.W. Wendlandt, H.G. Hecht, Reflectance Spectroscopy, Wiley Interscience, New York, 1966.

[27] Y. Zhang, H. Li, S. Moricca, unpublished work.

[28] P.J. McGlinn, Y. Zhang, H. Li, T.E. Payne, Mat. Res. Soc. Symp. Proc. 985 (2008) 163.

[29] Y. Zhang, E.R. Vance, K.S. Finnie, B.D. Begg, M.L. Carter, Recent Advances in Actinide Science, Royal Society of Chemistry, 2006. p. 343.

[30] K.S. Finnie, Z. Zhang, E.R. Vance, M.L. Carter, J. Nucl. Mater. 317 (2003) 46.